Accelerated Publications

On the Solution Structure of the T4 Sliding Clamp (gp45)†

David Millar,‡ Michael A. Trakselis,§ and Stephen J. Benkovic*,||

Department of Molecular Biology MB-19, The Scripps Research Institute, 10550 North Torrey Pines Road, La Jolla, California 92037, MRC/Cancer Cell Unit, University of Cambridge, Hills Road, Cambridge, CB2 1XZ, United Kingdom, and Department of Chemistry, The Pennsylvania State University, 414 Wartik Laboratory, University Park, Pennsylvania 16802

Received August 2, 2004; Revised Manuscript Received August 18, 2004

ABSTRACT: Examination by time-resolved fluorescence spectroscopy of the trimeric bacteriophage T4 clamp protein labeled across its three subunit interfaces with a fluorescence resonance energy transfer (FRET) pair indicates that the clamp exists in just one state in solution, with one open and two closed interfaces. This is in contrast to what is observed in the X-ray crystal structure. The population distribution of the trFRET distance is bimodal, giving 67% as 17 Å and 33% as 42 Å. This leads to the conclusion that gp45 exists in an asymmetric open state in solution. The further increase in the separation of the FRET pair in the presence of the clamp loader and ATP may be ascribed to either further opening of the open interface or the opening of a closed interface. The ramifications for replisome remodeling by this pathway are discussed.

The X-ray crystal structures of the sliding clamps from bacteriophage T4 and RB69 (*4*, *5*), *Escherichia coli* (*6*), and yeast (*7*) have been solved. Despite limited primary sequence identity, all of these sliding clamps are circular, multimeric proteins with a central opening large enough to accommodate duplex DNA (*8*). Trimeric gp45 from T4 and dimeric β clamp from *E. coli* each have six domains with flexible connecting loops tethering these domains and are closed at all of the subunit interfaces. However, using a mutant form of gp45 (V163C/W199F), in which the introduced cysteine is derivatized with 7-diethyl amino-3-(4′-maleimidyl phenyl)-4-methylcoumarin (CPM),[1] we have measured a fluorescence resonance energy transfer (FRET) signal between CPM and Trp-92 located on the opposite side of the gp45 subunit interface (*2*, *3*). The FRET data were consistent with a model of gp45, having one open subunit interface, with a W92/V163C−CPM distance of 35−38 Å, and two closed subunit interfaces, with W92/V163C−CPM distances of 19 Å.[2] We proposed that the distances probably were the average of two equilibrating forms of gp45 in solution. We now describe measurements of the decay kinetics of the Trp-92 emission arising from fluorophore-labeled gp45 (V163−CPM, W199F) and show that they are consistent with only one state of gp45, with one open and two closed subunit interfaces. Given the absence of a closed form in solution, we have further examined the influence of the clamp loader (gp44/62) on the clamp protein.

MATERIALS AND METHODS

Time-Resolved Fluorescence Spectroscopy. The labeled gp45 was prepared as reported previously (*9*). The mutant gp44(K56A)/62 was prepared previously (*10*). Stopped-flow experiments were performed, and the measured values of FRET efficiency were converted to donor−acceptor distances as described in Trakselis et al. (*9*). Time-resolved fluorescence measurements were performed using the time-correlated single-photon-counting method. Samples were placed in a temperature-controlled housing at 20 °C and repetitively excited by short pulses (∼2 ps width, 1.87 MHz repetition rate) of vertically polarized laser light. The laser pulses were generated by a mode-locked titanium/sapphire laser (Coherent Mira) operating at 885 nm, the output from which was passed through a frequency-tripling system to generate 295 nm pulses for excitation. The resulting emission was collected at 90° to the excitation beam, collimated by a lens, and then passed through a polarizer oriented at the magic angle (54.7° from vertical). Fluorescence emission was monitored at 345 nm using a monochromator with a spectral band pass of 16 nm, and photons were detected by a microchannel plate photomultiplier (Hamamatsu R2809U-01). The photomultiplier output was processed with standard time-correlated single-photon-counting electronics. Fluorescence decay curves were collected in 4096 channels with a time increment of 10 ps/channel. Data collection was terminated when 40 000 counts were in the peak channel of the decay curve. The instrument response function was collected at 295 nm using light scattered from a dilute suspension of nondairy coffee creamer.

† This work was supported by NIH Grants GM013306 (to S.J.B.) and GM44060 (to D.P.M.).

* To whom correspondence should be addressed. Telephone: (814)-865-2882. Fax: (814)865−2973. E-mail: sjb1@psu.edu.

‡ The Scripps Research Institute.

§ University of Cambridge.

|| The Pennsylvania State University.

[1] Abbreviations: CPM, 7-diethyl amino-3-(4′-maleimidyl phenyl)-4-methylcoumarin; FRET, fluorescence resonance energy transfer.

[2] The sequence of gp45 was corrected by Miller et al. (*1*). W91 and V162 in previously published papers (*2*, *3*) are now W92 and V163.

10.1021/bi048349c CCC: $27.50
Published on Web 09/04/2004

Time-Resolved Fluorescence Data Analysis. Time-resolved fluorescence data were analyzed by a standard reconvolution procedure (*11*) using nonlinear least-squares regression (*12*). The fluorescence intensity decay of Trp-92 in unlabeled V163C/W199F gp45 (donor-only decay) was fit to a sum of exponentials (eq 1), where α_i is the amplitude of each

$$K(t) = \sum_{i=1}^{N} \alpha_i \, e^{-t/\tau_i} \quad (1)$$

component and τ_i is the corresponding decay time. The minimum number of components required for best fit was determined by successively incrementing the value of N in eq 1 and evaluating the goodness of fit using the reduced χ^2 criterion. The mean fluorescence lifetime was calculated according to eq 2. Equation 1 was also used to analyze the

$$\langle \tau \rangle = \sum_{i=1}^{N} \alpha_i \tau_i \quad (2)$$

fluorescence intensity decay of Trp-92 in CPM-labeled V163C/W199F gp45. The FRET efficiency, E, was calculated from the mean donor lifetimes in the absence, $\langle \tau_D \rangle$, or presence, $\langle \tau_{DA} \rangle$, of the acceptor, according to eq 3.

$$E = 1 - \frac{\langle \tau_{DA} \rangle}{\langle \tau_D \rangle} \quad (3)$$

The donor decay in the presence of the acceptor was also analyzed using a model of donor−acceptor distance distributions

$$I_{DA}(t) = \sum_k f_k \int P_k(R) \sum_{i=1}^{N} \alpha_i \exp\left(- \frac{t}{\tau_i} \left[1 + \left(\frac{R}{R_0} \right)^6 \right] \right) dR \quad (4)$$

where R_0 is the critical transfer distance from the Trp-92 donor to the CPM acceptor and $P(R)$ is the probability distribution describing the donor−acceptor distance, R. The donor−acceptor distance distribution was represented by a weighted Gaussian function

$$P_k(R) = c_k \exp(- a_k (R - b_k)^2) \quad (5)$$

where a_k and b_k are adjustable parameters that together describe the shape of the distribution and c_k is a normalization constant. The intrinsic donor lifetimes and decay amplitudes in eq 4 were fixed at the values determined from the donor-only decay, while the shape parameters a_k and b_k in eq 5 were optimized for best fit. Donor decays were analyzed according to eq 4 using both unimodal ($k = 1$) and bimodal ($k = 2$) distance distributions. The Förster distance for the tryptophan/CPM pair is 31 Å (*2*).

RESULTS AND DISCUSSION

A mutant form of gp45 (V163C/W199F) containing a single tryptophan residue (Trp-92) and a unique cysteine residue suitable for attachment of a complementary FRET acceptor, CPM, has been described previously (*2*, *3*). In a gp45 trimer, a donor and acceptor lie on opposite sides of each of the three subunit interfaces, allowing for the measurement of the distance across these interfaces by means of FRET. In previous steady-state experiments, FRET was observed by measuring the sensitized acceptor emission arising from excitation of the tryptophan donor (*2*). Here, we extend these measurements by quantifying the effect of the CPM acceptor on the fluorescence decay kinetics of the tryptophan donor. In principle, time-resolved measurements can reveal different donor−acceptor distances across each of the three subunit interfaces.

Tryptophan was excited at 295 nm by a short laser pulse (ca. 2 ps), and the decay of the resulting emission at 345 nm was recorded by time-correlated single-photon counting. In the absence of the CPM acceptor, the Trp-92 emission exhibited a biexponential decay, with a mean fluorescence lifetime of 2.93 ns (individual lifetimes of 3.61 and 1.57 ns, with corresponding decay amplitudes of 0.756 and 0.244, respectively). Generally, the existence of multiple fluorescence decay components for a single tryptophan residue is attributed to different rotamers of the indole side chain (*13*). In the presence of the CPM acceptor, the mean fluorescence lifetime of Trp-92 was reduced to 1.01 ns and the intensity decay required 3 decay components for best fit. It should be noted that the increased complexity of the donor decay in the presence of the acceptor does not necessarily indicate any change in the distribution of side-chain rotamers, rather it reflects significant heterogeneity in the donor−acceptor distance (see below). Regardless, the overall FRET efficiency E can be estimated from the mean donor lifetimes in the presence and absence of acceptor, according to eq 3. The resulting value, $E = 0.655$, is in good agreement with previous steady-state measurements of sensitized acceptor emission (*2*).

To extract distance information, the decay of Trp-92 in acceptor-labeled protein was analyzed using a model of donor−acceptor distance distributions (eq 4). For these fits, the intrinsic donor lifetimes and decay amplitudes were kept fixed at the values determined above for the donor-only protein. The tryptophan donor decay (Figure 1A) was initially fitted with a single Gaussian distribution of donor−acceptor distances ($k = 1$ in eq 4), but the resulting fit was poor, as indicated by the value of the reduced χ^2 parameter ($\chi_r^2 = 12.0$) and a nonrandom distribution of weighted residuals (not shown). However, a good fit was obtained using a bimodal distance distribution ($k = 2$ in eq 4), which is reflected in both the reduced χ^2 value ($\chi_r^2 = 1.4$) and the weighted residuals (shown in Figure 1B). The corresponding donor−acceptor distance distribution is shown in Figure 1C. The major species, accounting for 67 ± 13% of the total donor population, has a mean donor−acceptor distance of 16.7 ± 3.9 Å and a distribution width (full width at half-maximum probability) of 11.7 ± 0.9 Å. The minor species (33%) has a mean donor−acceptor distance of 42.2 ± 3.0 Å and a distribution width of 19.6 ± 0.9 Å.

The results of the donor decay analysis indicate that two gp45 subpopulations are present in solution, with significantly different tryptophan−CPM distances. Each distance is described by a distribution rather than a single value, presumably because of the conformational flexibilities of the tryptophan side chain and the linker between the CPM moiety and the labeled cysteine residue. In principle, the observed heterogeneity in the tryptophan−CPM distance could arise from (1) incomplete labeling of the introduced cysteine with CPM, (2) a mixture of monomeric and trimeric gp45 species,

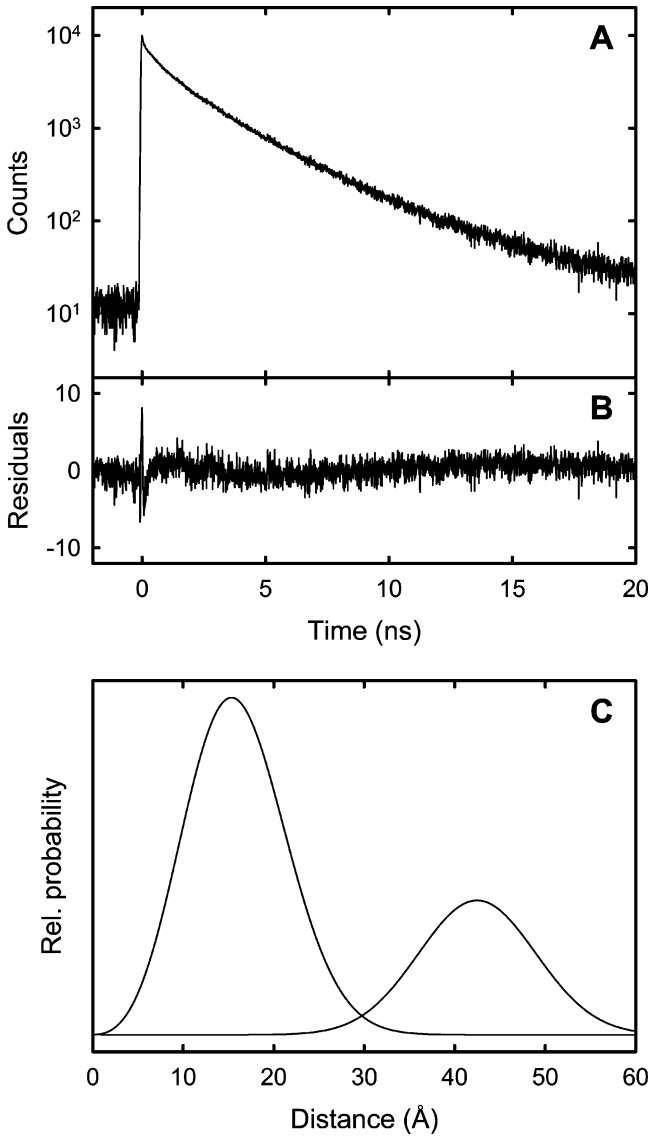

FIGURE 1: Tryptophan fluorescence intensity decay and donor−acceptor distance distribution analysis. (A) Time-resolved intensity decay of Trp-92 in the CPM−V163C/W199F gp45 construct. The excitation and emission wavelengths are 295 and 345 nm, respectively. (B) Weighted residuals obtained from fitting the intensity decay using a bimodal distribution of donor−acceptor distances. (C) Corresponding donor−acceptor distance distribution. The major species (67 ± 13%) has a mean donor−acceptor distance of 16.7 ± 3.9 Å and a distribution width (full width at half-maximum probability) of 11.7 ± 0.9 Å. The mean distance and distribution width of the minor species are 42.2 ± 3.0 and 19.6 ± 0.9 Å, respectively.

or (3) different subunit distances within a single gp45 trimer. The first possibility is ruled out by measurements of the stoichiometry of CPM labeling, which indicate 100% labeling of gp45 (results not shown). To exclude the second possibility, the time-resolved FRET analysis was repeated across a range of gp45 concentrations from 2 to 20 μM. The recovered fractions of the two donor−acceptor species were constant across this range, arguing against the possibility that the long distance (low FRET) species actually represents a population of gp45 monomers. Hence, the most likely explanation of our results is that the donor−acceptor distances across the three subunit interfaces of a single gp45 trimer are inequivalent.

In a previous steady-state FRET study (*2*), all three of the subunit interfaces were constrained in a closed conformation by the presence of disulfide linkages. The resulting FRET efficiency ($E = 0.95$) indicated a tryptophan−CPM distance of 19 Å at each interface. However, a significantly lower FRET efficiency ($E = 0.70$) was measured for an unconstrained gp45 trimer. This discrepancy could indicate that the disulfide cross links alter the natural distance across each of the subunit interfaces. Alternatively, one of the subunit interfaces may open in the unconstrained gp45 trimer, with a correspondingly longer distance between the tryptophan donor and CPM acceptor. The previous steady-state data could not distinguish between these two possibilities. However, the present trFRET results clearly show that two different subunit distances are present in the gp45 trimer. Significantly, the short distance recovered by trFRET (16.7 ± 3.9 Å) agrees well with the value obtained previously for the constrained gp45 trimer, indicating that this distance reflects closed subunit interfaces. The longer distance (42.2 ± 3.0 Å) corresponds to an open interface. Hence, the trFRET data directly reveal the presence of both open and closed subunit interfaces in the gp45 trimer and quantify the tryptophan−CPM distance in each case.

The previous steady-state data could not resolve whether an open interface was present in all or just some of the gp45 trimers. This question is also answered by the present trFRET results. First, we note that a trimer of three gp45 subunits can be either fully closed or have one (and only one) open interface. If fully closed, each of the tryptophan donors will be associated with a short donor−acceptor distance. In the open form, two out of three tryptophans will have a short donor−acceptor distance. Hence, the fractional population of the short-distance species will be 100 or 66.7% for the closed and open forms, respectively. For a mixture of the two forms, the fractional population lie between these values. Experimentally, we find that 67 ± 13% of tryptophan donors are associated with the short distance. Hence, our results indicate that all gp45 trimers have one open subunit interface in solution, although we cannot rule out the presence of a small population of fully closed rings in view of the experimental uncertainty in the recovered fraction. This behavior is different than what is observed in the X-ray crystal structure, where all three interfaces are fully closed (*4*). A model of the gp45 clamp based on our trFRET results is shown in Figure 2.

Given the open form of the gp45 clamp protein in solution, the immediate question that arises is the role of the clamp-loader protein, gp44/62, which consists of four gp42 subunits and one gp62 and its requirement for ATP hydrolysis to function (*14*). A comparison to the *E. coli* clamp loader, the γ complex, whose structure has been determined, is instructive (*15*). In the γ complex, the subunits are arranged in a circular heteropentamer comprised of three γ subunits that bind ATP, a δ subunit that binds to and opens the clamp protein, β, and a δ' subunit that modulates the interaction between γ and β. By sequence comparison, it is apparent that gp44/62 lacks a δ' subunit. The opening of the β ring (there is no evidence for an open form in solution) can surprisingly be effected by δ alone (*16*) or in the presence of ADP (*17*), leading to the experimentally supported conclusion that the three equivalents of ATP hydrolyzed by the γ complex in the overall process of loading the β protein

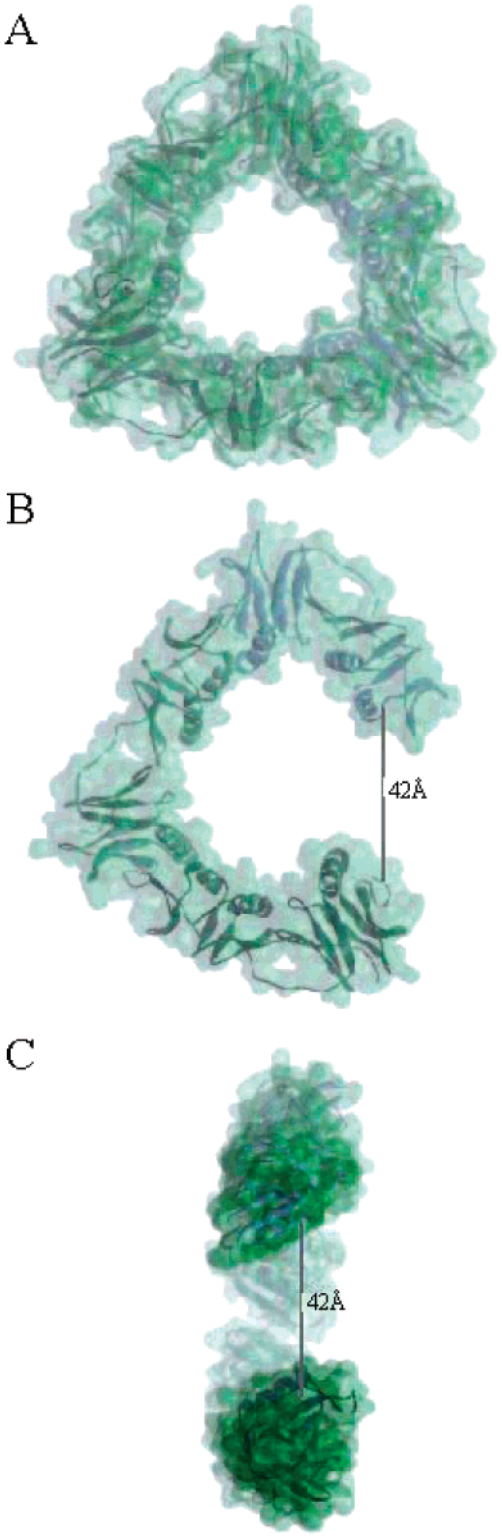

FIGURE 2: Ribbon diagrams with added surfaces of gp45. (A) Crystal structure of gp45. (B) Solution structure of gp45 showing a static open interface of ~42 Å and (C) rotated 90° around the *y* axis.

onto primed DNA allow the dissociation of the γ complex from β already loaded onto DNA (*18*, *19*).

On the basis of previous pre- and steady-state kinetic studies (*2*, *3*, *9*, *20*), we suggested that ATP hydrolysis by the T4 clamp loader accompanies the formation of a gp44/62·gp45 complex, competent for clamp loading. Using CPM-labeled V163C/W199F gp45, one could identify steps within the kinetic sequence for clamp loading with opening/closing

Scheme 1

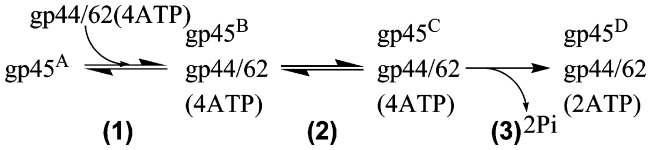

of the gp45 ring (Scheme 1). Notably, the transition from state C → D is associated with an increase in the subunit interface distance. Previously, we found that the clamp loader does not open the clamp further in the presence of ADP or ATγS (*21*). To confirm that ATP hydrolysis is required to open the clamp, we monitored clamp opening in the presence of a catalytically inactive clamp loader (Gp44(K56A)/62) (*10*) and a slow tight binding inhibitor (AlF_4). Gp44(K56A)/62 was found to bind but not hydrolyze ATP.

Notably, ADP (K_i = 20 μM) and ADP/AlF_4 in the presence of gp44/62 or gp44 (K65A)/62 do not promote the transition from state C → D. The calculated subunit interface distance of gp45 was <40 Å in all of the following conditions: gp44/62/ADP, gp44/62/ATγS, gp44/62/ADP/AlF_4, and gp44(K56A)/62/ADP/AlF_4. Only the inclusion of ATP opened the clamp interface to >45 Å. We conclude that, unlike the γ complex and despite the presence of an open form of gp45, this clamp loader functions through ATP hydrolysis (not simply binding) to load the clamp onto DNA.

In the present study, we have also shown that gp45 is statically open in solution of a distance large enough to accommodate dsDNA. The question, of course, arises as to why a clamp loader is needed in the first place. One possibility is that the clamp loader acts to further increase the separation at the open subunit interface upon hydrolysis of ATP. The enlarged opening would provide for a greater chance of the clamp docking onto DNA, akin to throwing a horseshoe around a pole. Alternatively, the opening may be blocked by another replisome component, in which case the clamp loader may open one of the other subunit interfaces to load the complex onto DNA. In fact, there is evidence that gp45 and gp43 polymerase readily form a binary complex in solution, most likely through the interaction of the C terminus of gp43 with the open subunit interface in gp45 (*21*). Such a complex can be loaded onto DNA by the clamp loader to yield an active holoenzyme (*22*). Loading of the clamp−polymerase complex also suggests a solution to the problem of delivering the clamp to the 3′ terminus of the primer through its recognition by the polymerase. Although this pathway for holoenzyme formation proceeds some 60-fold slower than the one proceeding through a clamp−clamp-loader complex, it may be predominant under certain conditions.

In view of the preceding discussion, it follows that the observed increase in the subunit/subunit separation in gp45 during clamp loading may reflect the opening of one of the closed interfaces of the clamp or an additional separation of the open interface. The opening of a second interface on the clamp protein by the clamp loader not only provides a way to load the complex onto DNA but also to drive complex formation with an additional protein, such as the primase or helicase accessory protein, when the holoenzyme is carrying out lagging strand synthesis. This mechanism will be the subject of a future communication. The kinetically preferred pathway, loading of the clamp protein by the clamp loader onto DNA followed by complexation by the polymerase, may

also require the opening of a second subunit interface rather than further separation of the open one. Distinguishing between the two different models of clamp opening is not possible with our current FRET techniques. Both the T4 clamp loader and clamp protein possess differing structural composition (clamp loader) and physical properties (clamp) than their *E. coli* counterparts, and the mechanistic differences may reflect a less evolved but nonetheless efficient mode of clamp loading.

NOTE ADDED AFTER ASAP POSTING

This paper was inadvertently posted on the Internet on 09/04/04. There is a change to be made in the seventh paragraph of the Results and Discussion. The second mention of ref *14* was changed to ref *15*. The correct version was reposted on the Internet on 09/13/04.

REFERENCES

1. Miller, E. S., Kutter, E., Mosig, G., Arisaka, F., Kunisawa, T., and Ruger, W. (2003) Bacteriophage T4 genome, *Microbiol. Mol. Biol. Rev. 67*, 86−156.
2. Alley, S. C., Shier, V. K., Abel-Santos, E., Sexton, D. J., Soumillion, P., and Benkovic, S. J. (1999) Sliding clamp of the bacteriophage T4 polymerase has open and closed subunit interfaces in solution, *Biochemistry 38*, 7696−7709.
3. Alley, S. C., Abel-Santos, E., and Benkovic, S. J. (2000) Tracking sliding clamp opening and closing during bacteriophage T4 DNA polymerase holoenzyme assembly, *Biochemistry 39*, 3076−3090.
4. Moarefi, I., Jeruzalmi, D., Turner, J., O'Donnell, M., and Kuriyan, J. (2000) Crystal structure of the DNA polymerase processivity factor of T4 bacteriophage, *J. Mol. Biol. 296*, 1215−1223.
5. Shamoo, Y. and Steitz, T. A. (1999) Building a replisome from interacting pieces: Sliding clamp complexed to a peptide from DNA polymerase and a polymerase editing complex, *Cell 99*, 155−166.
6. Kong, X. P., Onrust, R., O'Donnell, M., and Kuriyan, J. (1992) Three-dimensional structure of the β subunit of *E. coli* DNA polymerase III holoenzyme: A sliding DNA clamp, *Cell 69*, 425−437.
7. Gulbis, J. M., Kelman, Z., Hurwitz, J., O'Donnell, M., and Kuriyan, J. (1996) Structure of the C-terminal region of p21-(WAF1/CIP1) complexed with human PCNA, *Cell 87*, 297−306.
8. Kelman, Z. and O'Donnell, M. (1995) Structural and functional similarities of prokaryotic and eukaryotic DNA polymerase sliding clamps, *Nucleic Acids Res. 23*, 3613−3620.
9. Trakselis, M. A., Alley, S. C., Abel-Santos, E., and Benkovic, S. J. (2001) Creating a dynamic picture of the sliding clamp during T4 DNA polymerase holoenzyme assembly by using fluorescence resonance energy transfer, *Proc. Natl. Acad. Sci. U.S.A. 98*, 8368−8375.
10. Trakselis, M. A., Roccasseca, R., Yang, J., and Benkovic, S. J. (2003) Dissociative properties of proteins within the bacteriophage T4 replisome, *J. Biol. Chem.* manuscript submitted.
11. Grinvald, A. and Steinberg, I. Z. (1974) On the analysis of fluorescence decay kinetics by the method of least-squares, *Anal. Biochem. 59*, 583−598.
12. Bevington, P. R. (1969) *Data Reduction and Error Analysis for the Physical Sciences*, McGraw−Hill Book Co., New York.
13. Dahms, T. E. and Szabo, A. G. (1997) Conformational heterogeneity in crystalline proteins: Time-resolved fluorescence studies, *Methods Enzymol. 278*, 202−221.
14. Mace, D. C. and Alberts, B. M. (1984) The complex of T4 bacteriophage gene 44 and 62 replication proteins forms an ATPase that is stimulated by DNA and by T4 gene 45 protein, *J. Mol. Biol. 177*, 279−293.
15. Jeruzalmi, D., O'Donnell, M., and Kuriyan, J. (2001) Crystal structure of the processivity clamp loader γ complex of *E. coli* DNA polymerase III, *Cell 106*, 429−441.
16. Turner, J., Hingorani, M. M., Kelman, Z., and O'Donnell, M. (1999) The internal workings of a DNA polymerase clamp-loading machine, *EMBO J. 18*, 771−783.
17. Stewart, J., Hingorani, M. M., Kelman, Z., and O'Donnell, M. (2001) Mechanism of β clamp opening by the δ subunit of *Escherichia coli* DNA polymerase III holoenzyme, *J. Biol. Chem. 276*, 19182−19189.
18. Snyder, A. K., Williams, C. R., Johnson, A., O'Donnell, M., and Bloom, L. B. (2004) Mechanism of loading the *Escherichia coli* DNA polymerase III sliding clamp: II. Uncoupling the β and DNA binding activities of the γ complex, *J. Biol. Chem. 279*, 4386-4393.
19. Williams, C. R., Snyder, A. K., Kuzmic, P., O'Donnell, M., and Bloom, L. B. (2004) Mechanism of loading the *Escherichia coli* DNA polymerase III sliding clamp: I. Two distinct activities for individual ATP sites in the γ complex, *J. Biol. Chem. 279*, 4376−4385.
20. Trakselis, M. A., Berdis, A. J., and Benkovic, S. J. (2003) Examination of the role of the clamp-loader and ATP hydrolysis in the formation of the bacteriophage T4 polymerase holoenzyme, *J. Mol. Biol. 326*, 435−451.
21. Alley, S. C., Trakselis, M. A., Mayer, M. U., Ishmael, F. T., Jones, A. D., and Benkovic, S. J. (2001) Building a replisome solution structure by elucidation of protein−protein interactions in the bacteriophage T4 DNA polymerase holoenzyme, *J. Biol. Chem. 276*, 39340−39349.
22. Sexton, D. J., Kaboord, B. F., Berdis, A. J., Carver, T. E., and Benkovic, S. J. (1998) Dissecting the order of bacteriophage T4 DNA polymerase holoenzyme assembly, *Biochemistry 37*, 7749−7756.

BI048349C